

Bandgap tunability in graphene via bag boundary conditions on Dirac quasispinors

Yusef Koohsarian^{1,*} and Ali Naji^{2,1,†}

¹*School of Physics, Institute for Research in Fundamental Sciences (IPM), P.O. Box 19395-5531, Tehran, Iran*

²*School of Nano Science, Institute for Research in Fundamental Sciences (IPM), P.O. Box 19395-5531, Tehran, Iran*

Using field-theoretic descriptions of low-energy excitations in graphene via massless Dirac quasispinors, we show that a generalized form of bag boundary conditions on quasispinor currents can be used to predict continuous bandgap tunability in narrow areas (nanolanes) of graphene. The model nanolanes are envisaged as quasi-one-dimensional areas between any pair of straight parallel lines drawn across the honeycomb lattice, with the quasispinor currents allowed to partially permeate through the boundary lines. We show that such a construction predicts metalizable armchair and zigzag nanolanes, whose bandgaps can be decreased down to zero by decreasing the mismatch between the boundary permeabilities, as well as insulating nanolanes, whose bandgaps can be made significantly larger than those of graphene nanoribbons. The cases of graphene nanoribbons follow from our model in the limit of impermeable (no-flux) boundaries. Unlike previous implementations of no-flux bag boundaries, our formulation accurately reproduces the tight-binding results for the nanoribbon bandgap down to nanoribbon widths of only a couple of lattice spacing, even as the nanolane description does not include the edge-states of zigzag nanoribbons.

I. INTRODUCTION

The discovery of graphene—the prominent single-layer honeycomb lattice of carbon atoms^{1–4}—and its derivatives have made a significant impact on a wide range of technological applications^{5–7}, thanks to their remarkable transport, optical and mechanical properties. One of the key physical aspects of monolayer graphene is its gapless spectra of low-energy (electron-hole) excitations. These emerge as massless Dirac quasispinors^{8–13}, bringing the low-energy physics of graphene into close analogy with the quantum field theory of Dirac spinors (notwithstanding the fact that the speed of light is replaced by the Fermi velocity and a true Lorentz invariance is absent in graphene). Massless Dirac quasispinors are responsible for some of the most exotic phenomena in graphene, including the anomalous quantum Hall effect^{14–16} and Klein tunneling^{17–19}, being itself a long-standing prediction for Dirac spinors in quantum field theory^{20,21}. These have motivated a substantial interest in field-theoretic formulations of graphene physics in the recent past^{9,22,23}.

While unbounded graphene has thoroughly been considered within the field-theoretic context, its other realizations, such as graphene nanoribbons (GNRs) have received less attention^{31,32,34,35}. GNRs have emerged as promising semiconducting materials with tunable bandgap in nanoelectronic applications, particularly at room temperature^{24–26}. They are realized with regular or irregular arrangements of carbon atoms on their side edges, with the most commonly studied cases being the fixed-width GNRs with regular, armchair and zigzag edge configurations. The low-energy spectrum of a GNR is found to be dependent on its width w and the edge configuration: Armchair GNRs turn out to be gapless for the width-subtype $w = (3m - 1)d$ and gapped for the width-subtypes $w = (3m - 2)d$ and $3md$, where m is a positive integer and d is the honeycomb lattice constant^{27–30}. Zigzag GNRs are predicted to have gapless (metallic) edge-states regardless of their width w .

The energy band of GNRs are customarily calculated using the tight-binding approach^{27–30}, where Dirichlet-type boundary conditions are imposed on the pertinent electronic wavefunctions at appropriate nanoribbon side edges (see, e.g., the detailed review in Ref.³⁰). The low-energy spectra of GNRs have recently been addressed within field-theoretic frameworks based on massless Dirac equations by imposing the so-called bag boundary conditions on quasispinor currents^{34–36}. Bag models—such as the celebrated MIT bag model^{41–44}—were proposed in quantum chromodynamics as a consistent route to confine Dirac spinors (quarks in hadrons) through no-flux conditions imposed on spinor currents along the surface normal of an assumed confining volume, resembling an impermeable ‘bag’^{46,47} (see also Ref.⁴⁸). In the case of armchair GNRs, a particular type of boundary conditions was devised for the corresponding Dirac equations by admixing the valleys at the edges of the armchair^{31,32}. This type of boundary conditions essentially circumvents the well-known inconsistencies of Dirichlet boundary conditions with the Dirac equations. It was later shown³⁶ that the proposed armchair boundary conditions in Refs.^{31,32} are indeed equivalent to the no-flux boundary conditions of bag models.

In this paper, we revisit the problem of bag boundary conditions for quasispinor confinement in graphene by placing it in a broader context. We draw on the conventional notion of graphene nanolanes (GNLs) that are defined as narrow quasi-one-dimensional areas of the honeycomb lattice confined between an arbitrary pair of parallel boundary lines. The boundary lines are supplemented with a *generalized* form of the bag boundary conditions by assuming that they can sustain finite *permeabilities* to Dirac quasispinor currents. We show that not only this simple construction can be used to reproduce the energy bandgap of GNRs as limiting cases of symmetric GNLs with zero boundary permeability, it can also be used to make other remarkable predictions. These include ‘metalizable’ armchair and zigzag GNLs, whose bandgaps

(unlike their nanoribbon counterparts) can continuously be tuned and reduced to zero. This is enabled by varying the difference in the permeabilities of the two boundaries as the relevant control parameter of the system. We also predict insulating armchair and zigzag GNLs, whose bandgaps can significantly exceed typical GNR values.

Despite the continuum nature of our approach, its bandgap predictions in the armchair-GNR limit turn out to agree quite well with those of the tight-binding model^{27–30} even as the width is reduced to just a couple of lattice spacings (as such, we also clarify the source of deviations shown by the results in Ref.³¹ as being due to an overlooked width offset). In the zigzag-GNR limit, our model predicts vanishing gap (regardless of the nanoribbon width) in agreement with the tight-binding approach. The model incorporates no physical (lattice termination) edges and, hence, no zigzag edge-states, which themselves appear to signify the Dirichlet boundary conditions used in the GNR context within both tight-binding^{30,33} and massless Dirac formulations³¹.

In Section II, we provide a brief background on Dirac quasispinors in graphene, followed by the discussion of the model predictions for GNLs with generalized armchair and zigzag boundaries in Sections III A and III B, respectively, and concluding remarks in Section IV.

II. MODEL DESCRIPTION

Quasispinor representation of electronic states in an unbounded monolayer graphene follows standardly from a tight-binding formulation of in-plane π -electron hopping between nearest-neighbor carbon atoms. Thanks to its two-dimensional (2D) honeycomb lattice, incorporating two triangular sublattices, an undoped monolayer displays conduction and valence energy bands in the 2D reciprocal (\mathbf{k}) space that meet at six individual Dirac points at the corners of the first Brillouin zone. Only two of the Dirac points turn out to be independent and can suitably be chosen as $\mathbf{K}_\pm = (0, \pm \frac{4\pi}{3d})$, where $d \simeq 2.46 \text{ \AA}$ is the lattice spacing. The low-energy excitations of wavevector $\mathbf{q} = \mathbf{k} - \mathbf{K}_\pm$, measured from the Dirac points, are found to obey independent massless Dirac equations, with identical linear energy dispersions, $\epsilon_{\mathbf{q}} = \lambda \hbar \omega_{\mathbf{q}}$, where $\omega_{\mathbf{q}} = v_F |\mathbf{q}|$ and $v_F \simeq 10^6 \text{ m/s}$ is the Fermi velocity. While the subscripts \pm are used to denote the valley index associated with \mathbf{K}_\pm , the dispersion relation itself adopts positive and negative solutions identified by the (conduction versus valence) band index, $\lambda = \pm 1$, which is intrinsically related to the sublattice (or quasispin) index, not being explicitly shown here. At each Dirac point, the probability amplitudes of Bloch wavefunction on the two underlying sublattices can be combined into the 2-spinor fields $\psi_{\pm, \mathbf{q}}(\mathbf{r})$, which themselves combine into a 4-spinor $\Psi_{\mathbf{q}}(\mathbf{r}) = (\psi_{+, \mathbf{q}}(\mathbf{r}), \psi_{-, \mathbf{q}}(\mathbf{r}))^T$, fulfilling

$$i v_F \gamma^0 \gamma^a \partial_a \Psi_{\mathbf{q}}(\mathbf{r}) = \omega_{\mathbf{q}} \Psi_{\mathbf{q}}(\mathbf{r}); \quad a = 1, 2 \quad (1)$$

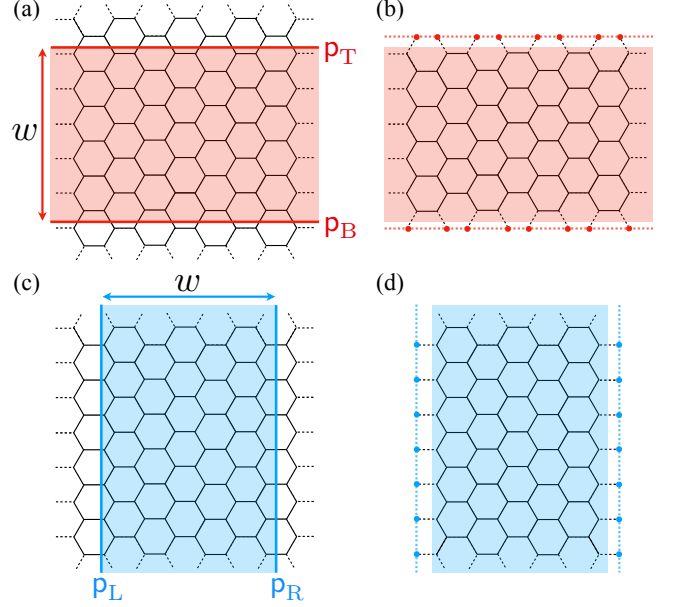


FIG. 1. (a) and (c): Schematic views of the model construction being referred to as graphene nanolane (GNL); here with armchair and zigzag edges, respectively, and with finite permeabilities ($p_{B,T}$ and $p_{L,R}$) to quasispinor currents at the boundaries. (b) and (d): Corresponding cases of armchair and zigzag graphene nanoribbons (GNRs), where the physical boundaries (red and blue dotted lines, respectively) are shifted by a total offset of d from those of their respective GNLs (colored areas) in each case and the permeabilities are set to zero ($p_{B,T} = p_{L,R} = 0$).

where γ^a defined using Pauli matrices as^{37,38}

$$\gamma^0 = \begin{pmatrix} \sigma_3 & 0 \\ 0 & \sigma_3 \end{pmatrix}, \gamma^1 = \begin{pmatrix} i\sigma_1 & 0 \\ 0 & i\sigma_1 \end{pmatrix}, \gamma^2 = \begin{pmatrix} i\sigma_2 & 0 \\ 0 & -i\sigma_2 \end{pmatrix}. \quad (2)$$

For brevity, we henceforth drop the subscript \mathbf{q} . The quasispinor currents, $J^\nu = \Psi^\dagger \gamma^0 \gamma^\nu \Psi$ ($\nu = 0, 1, 2$), involve the spatial parts $J^a = J_+^a + J_-^a$, with $J_\pm^a = \psi_\pm^\dagger i\sigma_3 \sigma_a \psi_\pm$ each incorporating electron/hole contributions.

In principle, any external source that could break the isotropy of the π -electron distribution in monolayer graphene would produce an in-plane boundary condition for quasispinors. In the case of GNRs, the no-flux bag boundary conditions à la standard bag models^{41–48} that require zero current, $\mathbf{J}_\pm = (J_\pm^1, J_\pm^2)$, in the normal direction at nanoribbon side edges, are written as

$$J_\pm^\perp \equiv \mathbf{J}_\pm \cdot \hat{\mathbf{n}} = 0, \quad (3)$$

where $\hat{\mathbf{n}} = (n_1, n_2)$ is the unit normal at each of the boundaries.

The generalized form of bag boundaries are introduced here within the construct of GNLs, defined as any area bounded by two arbitrary straight and parallel lines drawn on a graphene sheet; see panels a and c in Fig. 1. We shall specifically consider armchair (zigzag) GNLs by setting the boundary lines parallel to the hexagonal

sides (vertices) in the honeycomb lattice; e.g., for a GNL of width w , we conventionally choose the boundary positions as $y = \mp w/2$ ($x = \mp w/2$). Needless to say that the key difference here with armchair and zigzag GNRs is in the arbitrary choice of the boundary positions that can be varied continuously.

Each GNL boundary line is characterized by *permeability coefficients* \mathbf{p}_\pm associated with ψ_\pm ; hence, the generalized bag boundary conditions

$$J_\pm^\perp = \mathbf{p}_\pm. \quad (4)$$

The boundary permeabilities can generally be functions of the wavevector. Yet, in the specific geometry considered, we assume that they can be approximated as constants near the Dirac points. For simplicity, we drop the subscripts \pm and use ψ to denote ψ_\pm , noting that, due to time-reversal symmetry, the forthcoming calculations can similarly be repeated for either of the fields.

III. RESULTS

A. Armchair GNLs

For an armchair GNL, Eq. (4) can be written at the bottom (B) and top (T) boundaries as

$$\psi^\dagger \sigma_1 \psi|_{y=-w/2} = \mathbf{p}_B, \quad \psi^\dagger \sigma_1 \psi|_{y=w/2} = \mathbf{p}_T, \quad (5)$$

where we have used $\sigma_3 \sigma_2 = -i\sigma_1$, and denoted the boundary permeabilities by \mathbf{p}_B and \mathbf{p}_T . Equation (1) can be solved inside the GNL region ($|y| < w/2$) as

$$\psi \propto e^{iq_\parallel x} [\alpha e^{iq_\perp y} + \beta e^{-iq_\perp y}], \quad (6)$$

where α and β are constant 2-spinors, and $q_{\parallel,\perp}$ are the longitudinal/transverse components of \mathbf{q} . Equation (5) implies $(\alpha^\dagger \sigma_1 \beta + \beta^\dagger \sigma_1 \alpha) \sin(q_\perp w) = \mathbf{p}_T - \mathbf{p}_B$, or

$$\sin(q_\perp w) = \Delta, \quad (7)$$

where $\Delta \equiv \rho_T - \rho_B$, and the normalized coefficients $\rho_{B,T} \equiv \mathbf{p}_{B,T}/(\alpha^\dagger \sigma_1 \beta + \beta^\dagger \sigma_1 \alpha)$, with $0 \leq \rho_{B,T} \leq 1$, give the permeation probability amplitudes at the boundaries. By analogy, $\rho_{B,T}$ could be thought of as generalized dielectric responses of the boundaries, such that $\rho_{B,T} = 0$ and 1 will be reminiscent of ideally insulating (vacuum) and ideally polarizable (perfect metal) boundaries; hence, making Δ analogues to the dielectric jump parameter in the electrostatic context. Note also that $0 \leq |\Delta| < 1$ covers all realizable cases in the present context.

The permissible values of $q_{\perp,n}$ can be obtained from Eq. (7) and are standardly indexed by the integer $n = 0, \pm 1, \pm 2, \dots$; hence, the permissible wavevectors $\mathbf{k} = (k_\parallel, k_\perp)$ in the first Brillouin zone, with real-valued $k_\parallel = q_\parallel$ and discrete set $k_{\perp,n} = 4\pi/(3d) + q_{\perp,n}$, where

$$k_{\perp,n} = \frac{\pi}{w} \left[n + \frac{4}{3} \left(\frac{w}{d} \right) + \frac{1}{\pi} \sin^{-1} |\Delta| \right], \quad (8)$$

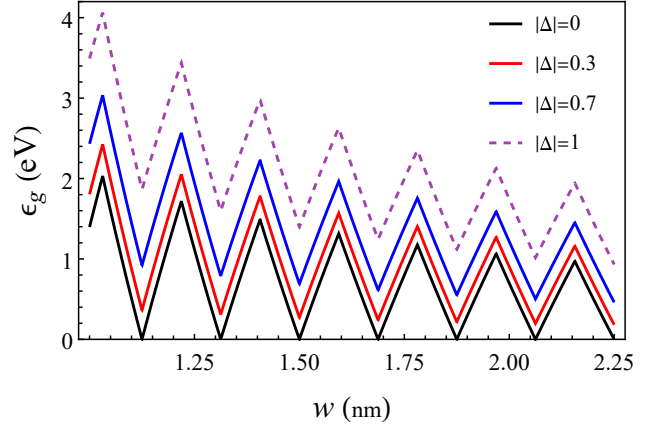


FIG. 2. Energy bandgap, ϵ_g , of armchair GNL as a function of its width w for different values of $|\Delta|$, as indicated on the graph. The sharp valleys represent metalizable GNLs. In these cases, ϵ_g is locally the smallest.

The low-energy spectra of an armchair GNL then follows as $E_n(k_\parallel) = \pm \hbar v_F \sqrt{k_\parallel^2 + k_{\perp,n}^2}$, with the bandgap

$$\frac{\epsilon_g}{\hbar v_F} = \frac{2\pi}{w} \begin{cases} \left| \frac{4}{3} \left(\frac{w}{d} \right) - \ell \right| + \frac{1}{\pi} \sin^{-1} |\Delta| & : \ell \leq \frac{4}{3} \left(\frac{w}{d} \right) < \ell + \frac{1}{2} \\ \left| \frac{4}{3} \left(\frac{w}{d} \right) - \ell - 1 \right| + \frac{1}{\pi} \sin^{-1} |\Delta| & : \ell + \frac{1}{2} \leq \frac{4}{3} \left(\frac{w}{d} \right) < \ell + 1, \end{cases} \quad (9)$$

where ℓ is a *positive* integer. In Fig. 2 the gap function ϵ_g has been plotted as a function of w , and selected values of $|\Delta|$, including its limiting values. The key aspects of our predictions in Eq. (9) can be summarized as follows.

- (i) *Band universality*: For an armchair GNL with symmetric (identical) boundary conditions $\mathbf{p}_B = \mathbf{p}_T$, one has $\Delta = 0$. As a result, the predicted bandgap (8) and, in fact, the whole energy spectra, reduce to those of an armchair GNR, *regardless* of the boundary permeability (note that the two cases of a symmetric GNL and a corresponding GNR remain physically separate, given that the latter case is further specialized as $\mathbf{p}_{B,T} = 0$). The low-energy excitations of a symmetric GNL thus display *universality* relative to the quasispinor currents at the boundaries. This is a direct consequence of coexisting time-reversal and parity-mirror symmetries. The time-reversal symmetry of the underlying graphene Dirac model ensures block-diagonal forms for the Hamiltonian and the corresponding γ -matrices (2), and allows one to impose independent bag conditions on ψ_\pm . By accounting for next-nearest-neighbor electron hopping in the underlying tight-binding model^{9,10}, the Hamiltonian loses its block-diagonal form, breaking the time-reversal symmetry of the electron-hole energy bands. On the other hand, it is straightforward to show that under mirror transformation $y \rightarrow -y$, the quasispinor currents transform as $J^\perp(y) \rightarrow J^\perp(-y)$, which preserves the mirror symmetry only if the boundary conditions are symmetric. In the asymmetric case with noniden-

tical boundaries, the mirror symmetry is violated locally (near the boundaries); an effect that can be interpreted as unequal quasiparticle densities near the GNL boundaries.

- (ii) *Metalizable armchair GNLs*: Equation (9) predicts that, for GNLs of width $w = w_M \equiv 3\ell/16$ (sharp local minima in Fig. 2), ϵ_g is (locally) the smallest,

$$\frac{\epsilon_g}{\hbar v_F} = \frac{2}{w_M} \sin^{-1} |\Delta|, \quad (10)$$

while it can be adjusted through Δ . Thus, by decreasing the boundary mismatch, an initially insulating GNL with sizable bandgap can be ‘metalized’ as Δ is decreased to zero. These metalizable GNLs can be regarded as generalized forms of the metallic modes in GNRs (see iii)^{27–32}; however, to emphasize, the GNLs in question are tunable between insulating and metallic states even as the width is kept fixed; an effect that is precluded in metallic GNRs.

- (iii) *Specialization to armchair GNRs*: To reproduce the case of an armchair GNR, one uses no-flux bag boundaries^{41–48} $p_{B,T} = 0$. The boundary lines are placed at the nanoribbon edges with a total offset of d ; see panels b and d in Fig. 1 (also Fig. 2 of Ref.³⁰). Hence, we find a modified form of Eq. (7) as

$$\sin[(k_{\perp} - 4\pi/3d)(w_* + d)] = 0. \quad (11)$$

In armchair GNRs, the width varies over a discrete subset of values, $w_*/d = 3\ell \pm 1$ and 3ℓ ; see Refs.^{27–30}. For $w_*/d = 3\ell - 1$, one finds $k_{\perp,n} = n\pi/(w_* + d)$ and the energy band turns out to be gapless. For $w_*/d = 3\ell, 3\ell + 1$, one finds $k_{\perp,n} = n\pi/(w_* + d) + 4\pi/(3d)$, leading to an energy band with no gapless modes. There is a slight difference with the GNR results in Refs.^{31,32}, where the width of the confined area is taken as $w + d/2$ (instead of $w + d$), missing an offset of $d/2$. This overlooked offset^{31,32} however leads to doubly degenerate states for $w_*/d = 3\ell - 1$, in disagreement with the tight-binding results in Refs.^{27–30}. Our GNR expressions above expectedly agree with the tight-binding ones^{27–30} in the limit of large widths. Interestingly, however, the relative deviation from the tight-binding results in Ref.³⁰ turns out to be remarkably small, $|\Delta\epsilon_g|/\epsilon_g \lesssim 5\%$ for all w_* down to a single unit cell width. By comparison, the results in Ref.³¹ show significantly larger relative deviations for small GNR widths from those in Ref.³⁰ (e.g., up to around 30% for $w_* \simeq 1$ nm; see Fig. 5 therein) and better agreement is established therein only for significantly larger GNR widths. Such deviations at small GNR widths appear to be attributed to the shortcomings of the continuum model³¹. Our results, however, show that the continuum modeling can remain relatively accurate down to just a couple of lattice spacings, and the reported numerical deviations in Ref.³¹ are due to the aforementioned missing offset.

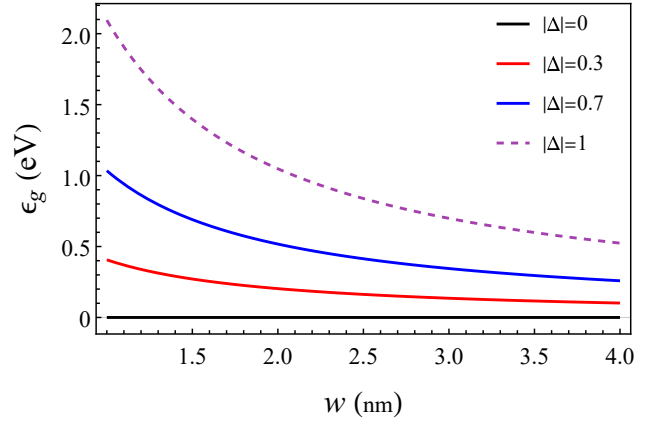


FIG. 3. Energy bandgap, ϵ_g , of zigzag GNL as a function of its width w for different values of $|\Delta|$, as indicated on the graph. As seen, a zigzag GNL is metalizable regardless of the choice of w , as the bandgap can be reduced to zero by decreasing Δ .

B. Zigzag GNLs

For a zigzag GNL, Eq. (4) at the left (L) and right (R) boundaries at $x = \mp w/2$ is written as

$$-\psi^\dagger \sigma_2 \psi|_{x=-w/2} = p_L, \quad -\psi^\dagger \sigma_2 \psi|_{x=w/2} = p_R, \quad (12)$$

and an equation for q_{\perp} (now denoting the x -component of \mathbf{q}) that would be similar to Eq. (7). Here, we have $k_{\perp} = q_{\perp}$, or

$$k_{\perp,n} = \frac{\pi}{w} \left[n + \frac{1}{\pi} \sin^{-1} |\Delta| \right], \quad (13)$$

with the same definition as given below Eq. (7), except that here the subscripts $\{B, T\}$ are replaced with $\{L, R\}$, respectively. The bandgap of a zigzag GNL is then given by the same expression as in Eq. (10), i.e.,

$$\frac{\epsilon_g}{\hbar v_F} = \frac{2}{w} \sin^{-1} |\Delta|, \quad (14)$$

where w now takes *arbitrary* values, and not just the discrete subset, denoted by w_M in the case of an armchair GNL. The zigzag GNL bandgap is shown in Fig. 3 as a function of the width w . Evidently, the continuous curves here pass through the metalizable states (sharp local minima) in Fig. 2.

A zigzag GNL with identical (nonidentical) boundaries will thus be metallic (insulator) and all states are metalizable, regardless of the choice of w . This is in agreement with the case of zigzag GNRs^{27–32}; however, unlike zigzag GNRs, zigzag GNLs have a closed-form expression for their low-energy spectra and possess no edge-states. The latter is expected as the GNLs have no actual lattice termination edges; also that edge-states appear to stem from Dirichlet boundary conditions imposed asymmetrically relative to the two different sublattices in the tight-binding calculations. As a consistency check, one

can confirm that Eq. (13) reproduces the analytical limit of large w from the tight-binding calculations³⁰.

IV. CONCLUDING REMARKS

Using an extended form of bag boundary conditions to allow for permeation of Dirac quasispinors through a pair of parallel boundary lines, forming a nanolane (GNL) over a graphene sheet, we predict robust energy spectra that feature highly tunable bandgaps. The bandgap tunability enters through the mismatch between the permeability coefficients of the two boundary lines of a GNL, which we study in its two armchair or zigzag subtypes. Remarkably, for a symmetric armchair GNL (identical boundary permeabilities), the energy spectra are found to be independent of the permeabilities. This type of GNL includes both metalized and insulating states, depending on the width. For asymmetric armchair GNLs (nonidentical boundary permeabilities), we find a discrete set of widths that produce metalizable states, whose bandgap can be reduced to zero, as the permeability mismatch is taken to zero. A zigzag GNL is, by contrast, always metalizable, regardless of the width.

Our model provides a field-theory-consistent route to bandgap calculation based on proper bag boundary conditions used for quasispinor currents; an approach that turns out to be relatively straightforward, yielding the bandgap in only a few steps of calculation, as compared with the tight-binding approach; see, e.g., Ref.³⁰. Also, while our model can be specialized to the case of GNRs, it can potentially be used to address a wider range of realistic situations involving nonideal (permeable) electronic confinement in graphene as well. For instance,

when a graphene sheet is suspended over a rectangular trench, the parallel boundary lines, created by the contacts between the sheet and the edges of the trench, may not necessarily be taken as ideally impermeable to quasispinor currents or as perfectly commensurate with the armchair and zigzag edges of a GNR.

Our analysis predicts bandgaps of considerably large magnitude; e.g., in the case of an armchair GNL of width $\gtrsim 1$ nm, bandgaps can be increased up to $\simeq 4$ eV, significantly larger than those obtained from Dirichlet tight-binding calculations for the corresponding GNR ($\lesssim 1$ eV)^{27–32}. As such, the GNL construction can be envisaged as a promising setting for electronic control in graphene-based nanosystems, with quantitative predictions that are expected to be fully accessible to experimental verification.

Finally, we note that the special case of no-flux bag boundaries can be implemented in its indirect form $i\gamma^a n_a \psi = \psi$, as considered in Refs.^{34,35}. Our analysis based on the direct form, $J^\perp = 0$, indicates that the two formulations may not be necessarily equivalent and it is the latter one that accurately reproduces the tight-binding results (the relevant GNR width-subtypes do not emerge in the former case^{34,35}). In the GNL context, the distinction between the two formulations of bag boundaries becomes even more apparent, as the boundaries exhibit finite permeabilities to quasispinor currents.

V. ACKNOWLEDGEMENT

Y.K. would like to thank Ahmad Shirzad and Kurosh Javidan for their support. The authors have no conflicts of interest to declare.

* yo.koohsarian@mail.um.ac.ir (corresponding author)

† a.naji@ipm.ir

¹ A. K. Geim, and K. S. Novoselov, Nature Materials 6, 183 - 191 (2007).

² A. K. Geim, Science 324, 5934, 1530-1534 (2009).

³ Novoselov, K. S., A. K. Geim, S. V. Morozov, D. Jiang, M. I. Katsnelson, I. V. Grigorieva, S. V. Dubonos, and A. A. Firsov, 2005, Nature 438, 197.

⁴ Zhou, S. Y., G.-H. Gweon, J. Graf, A. V. Fedorov, C. D. Spataru, R. D. Diehl, Y. Kopelevich, D.-H. Lee, S. G. Louie, and A. Lanzara, 2006, Nat. Phys. 2, 595.

⁵ Singh, V., Joung, D., Zhai, L., Das, S., Khondaker, S.I. and Seal, S., 2011. Progress in materials science, 56(8), pp.1178-1271.

⁶ A. N. Banerjee, Interface Focus 8, 20170056 (2018).

⁷ Sarma, S.D., Adam, S., Hwang, E.H. and Rossi, E., 2011. Reviews of modern physics, 83(2), p.407.

⁸ K. S. Novoselov, A. K. Geim, S. V. Morozov, D. Jiang, M. I. Katsnelson, I. V. Grigorieva, S. V. Dubonos, and A. A. Firsov, Nature 438, 197-200 (2005).

⁹ A. H. Castro Neto, F. Guinea, N. M. R. Peres, K. S. Novoselov, and A. K. Geim Rev. Mod. Phys., 2009, 81, 109.

¹⁰ D.S.L. Abergel, V. Apalkov, J. Berashevich, K. Ziegler, T. Chakraborty, 2010, Adv. Phys. 59:261-482.

¹¹ Novoselov, K.S., Fal, V.I., Colombo, L., Gellert, P.R., Schwab, M.G. and Kim, K., 2012. nature, 490(7419), pp.192-200.

¹² Backes, C., Abdelkader, A.M., Alonso, C., Andrieux-Ledier, A., Arenal, R., Azpeitia, J., Balakrishnan, N., Banszerus, L., Barjon, J., Bartali, R. and Bellani, S., 2020. 2D Materials, 7(2), p.022001.

¹³ Sarma, S.D., Adam, S., Hwang, E.H. and Rossi, E., 2011. Reviews of modern physics, 83(2), p.407.

¹⁴ Zhang, Y., Tan, Y.W., Stormer, H.L. and Kim, P., 2005. nature, 438(7065), pp.201-204.

¹⁵ Gusynin, V.P. and Sharapov, S.G., 2005. 95(14), p.146801.

¹⁶ Bolotin, K.I., Ghahari, F., Shulman, M.D., Stormer, H.L. and Kim, P., 2009. Nature, 462(7270), pp.196-199.

¹⁷ Beenakker, C.W.J., 2008, Reviews of Modern Physics, 80(4), p.1337.

¹⁸ Stander, N., Huard, B. and Goldhaber-Gordon, D., 2009. Physical review letters, 102(2), p.026807.

¹⁹ Jiang, X., Shi, C., Li, Z., Wang, S., Wang, Y., Yang, S., Louie, S.G. and Zhang, X., 2020, 370(6523), pp.1447-1450.

- ²⁰ Klein, O. Z. Phys. 53, 157-165 (1929).
- ²¹ Dombey, N., and Calogheracos, A., Phys. Rep. 315, 41-58 (1999).
- ²² Miransky, V.A. and Shovkovy, I.A., 2015. Physics Reports, 576, pp.1-209.
- ²³ Vozmediano, M.A., Katsnelson, M.I. and Guinea, F., 2010. Physics Reports, 496(4-5), pp.109-148.
- ²⁴ Li, X., Wang, X., Zhang, L., Lee, S. and Dai, H., 2008. science, 319(5867), pp.1229-1232.
- ²⁵ Wang, X., Ouyang, Y., Li, X., Wang, H., Guo, J. and Dai, H., 2008. Physical review letters, 100(20), p.206803.
- ²⁶ Schwierz, F., 2010. Nature nanotechnology, 5(7), p.487.
- ²⁷ Nakada, K., M. Fujita, G. Dresselhaus, and M. S. Dresselhaus, 1996, Phys. Rev. B 54, 17954
- ²⁸ Fujita, M., Wakabayashi, K., Nakada, K. and Kusakabe, K., 1996. Journal of the Physical Society of Japan, 65(7), pp.1920-1923.
- ²⁹ Ezawa, M., 2006. Physical Review B, 73(4), p.045432.
- ³⁰ Wakabayashi, K., Sasaki, K.I., Nakanishi, T. and Enoki, T., 2010. Sci. Technol. Adv. Mater. 11, 054504
- ³¹ Brey, L. and Fertig, H.A., 2006. Physical Review B, 73(23), p.235411.
- ³² Brey, L. and Fertig, H.A., 2007 , Physical Review B, 75(12), p.125434.
- ³³ Akhmerov A. R. and Beenakker C. W. J., 2008, Physical Review B 77, 085423
- ³⁴ Beneventano, C.G. and Santangelo, E.M., 2012, International Journal of Modern Physics: Conference Series (Vol. 14, pp. 240-249). World Scientific Publishing Company.
- ³⁵ Beneventano, C.G., Fialkovsky, I., Santangelo, E.M. and Vassilevich, D.V., 2014. The European Physical Journal B, 87(3), p.50.
- ³⁶ Beneventano, C.G., Fialkovsky, I., Nieto, M. and Santangelo, E.M. , 2018. Physical Review B 97, 155406.
- ³⁷ Fialkovsky, I.V. and Vassilevich, D.V., 2012. International Journal of Modern Physics A, 27(15), p.1260007.
- ³⁸ Fialkovsky, I.V. and Vassilevich, D.V., 2016. Modern Physics Letters A, 31(40), p.1630047.
- ³⁹ Son, Y.W., Cohen, M.L. and Louie, S.G., 2006. Physical review letters, 97(21), p.216803.
- ⁴⁰ Yang, L., Park, C.H., Son, Y.W., Cohen, M.L. and Louie, S.G., 2007. Physical Review Letters, 99(18), p.186801.
- ⁴¹ A. Chodos, R.L. Jaffe, K. Johnson, C.B. Thorn, V.F. Weisskopf, Phys. Rev. D 9, 3471-3495 (1974).
- ⁴² A. Chodos, R.L. Jaffe, K. Johnson, and C.B. Thorn, Phys. Rev. D 10, 2599 (1974).
- ⁴³ T.A. DeGrand, R.L. Jaffe, K. Johnson, and J. Kiskis, Phys. Rev. D L2, 2060 (1975).
- ⁴⁴ K. Johnson, Acta Phys. Polonica B 6, 865 (1975).
- ⁴⁵ P. Hasenfratz and J. Kuti, Phys. Rep. **40**, 75 (1978).
- ⁴⁶ A. W. Thomas and W. Weise, *The Structure of the Nucleon* (Wiley-VCH, Berlin, 2001).
- ⁴⁷ K.T. Hecht, *Quantum Mechanics* (Springer, New York, 2000).
- ⁴⁸ M. Berry and R. J. Mondragon, Proc. R. Soc. London A 412, 53 (1987).